JOURNAL OF MATERIALS SCIENCE 37 (2002) 2737–2745

Optical properties and local atomic order in non hydrogenated amorphous silicon carbonitride films

B. DOUCEY
SPCTS, Faculté des Sciences, UMR 6638, 123 Av. Albert Thomas, 87060 Limoges cedex, France

M. CUNIOT, R. MOUDNI
LPSC, CNRS, 1 place A.Briand, 92195 Meudon cedex, France

F. TÉNÉGAL
LURE, 91405 Orsay, France

J. E. BOURÉE
LPICM, CNRS UMR 7647, Ecole Polytechnique, F-91128, Palaiseau cedex, France

D. IMHOFF
LPS Université Paris-sud Orsay, Bât.510, F-91405 Orsay cedex, France

M. ROMMELUÉRE, J. DIXMIER
LPSC, CNRS, 1 place A.Briand, 92195 Meudon cedex, France
E-mail: jean.dixmier@cnrs-bellevue.fr

Non hydrogenated a-SiCN films have been prepared by Radio Frequency (RF) reactive sputtering of a SiC target in an $Ar + N_2$ plasma. The N content has been varied from 0 to 66 at.% of the sample composition. The structural and chemical orders have been investigated by X ray diffraction and X ray Absorption Near Edge Spectroscopy. The optical absorption properties of the films have been studied by transmittance measurements and by ellipsometry. A particular attention has been paid to the relation between the local order and the complex dielectric function. It has been shown that the atomic Short Range Order (SRO) rules the optical absorption while the index of refraction is dominated by the Medium Range Order (MRO). The as deposited samples have an heterogeneous microstructure containing zones where "mixed" tetrahedra Si $(C_{1-x}\ N_x)_4$ have been formed contiguously with other zones inside of which the basic SiC_4 and SiN_4 tetrahedra of the carbide and nitride are already present. The optical absorption edges of the SiCN deposits, remain close to the one of a-SiC, up to about 50% of nitrogen. The absence of hydrogen in a sample containing less than 1% of N allowed the study of the nitrogen induced relaxation of the network during heating treatements at 1200°C. The crystallization temperature of a-SiC is increased of about 200° and N atoms are located in substitution sites with a four fold coordinence. The optical gap widens after the annealing at 1200°C, from 1.6 to 2.4 ev which last value is in the same range that the gaps of non annealed a-SiC : H materials containing about 10% of hydrogen.

1. Introduction

Silicon carbide (SiC) and Silicon nitride (Si_3N_4) are excellent candidate materials for high temperature structural applications due to their strong convalent bonding. A considerable number of works have shown that by introducing SiC particles, platelets, or whiskers in a Si_3N_4 matrix, it is possible to modulate these material microstructures. This improves properties such as fracture toughness [1, 2], creep resistance [3, 4] or in the contrary the ductility [5, 6]. Composite materials derived from the association of Si_3N_4 and SiC has them made possible to widen the extend of the thermostructural properties of these ceramics and consequently their potential applications. With the same approach it is interesting to know how the optical and transport properties of a SiCN "alloy" could be influenced by the simultaneous presence of Si_3N_4 and SiC aggregates, in which Si_3N_4 is an insulator with a wide gap (5 eV) while SiC is a semiconductor with an intermediate gap (3 eV). The ultimate size effect is attained when the 3 kinds of atoms are mixed at the atomic size scale i.e, when the elementary tetrahedron vertices can be occupied

either by sp^3 bonded N or C atom (if Si is placed at the center of the tetrahedron). This hybridization of the local bonding between the 3 atoms cannot be realized within the frame of a phase diagram since no stable intermediate compounds $Si_xC_yN_z$ are known like in the Si-O-N system (the Si_2N_2O compound is stable). The "alloy" can be prepared only in the metastable amorphous state. This route has been followed in the recent past, thanks to the pyrolysis of organosilicon precursors and the organic-mineral transition. The hybridization of Si_3N_4 and SiC has been achieved mostly under the form of fibers, powders, but also of thin films to make hard coatings for wear enhancement and also for optical applications [7, 8]. The optical properties of SiCN ceramics have not been hitherto extensively studied. It has been observed that a few percent of N atoms embedded in the a-SiC : H matrix do not increase its optical gap [9]. This behaviour can be explained by supposing that N atoms are connected to near neighbours in the disordered network with a four fold coordination instead of three-fold like in the nitride [10]. They actually behave as dopants inducing an enhancement of the conductivity and photoconductivity. It implies, in the authors opinion, that N contributes to a decrease of the structural disorder. Following these previous approaches of the effect of hybridization on the properties of SiCN compounds, our purpose in the present study is to relate their optical characteristics to the local atomic order. We shall pay also a special attention to the early stages of the decomposition of the metastable SiCN hybrid.

2. Preparation

The amorphous $Si(C_x\ N_{1-x})$ thin films have been prepared by RF magnetron sputtering of a Si or SiC target in a $Ar + N_2$ gas mixture. Contrary to most other preparation techniques using organo-Silicon precursors (CVD, PECVD, Reactive sputtering in Ar with gases etc.), which necessarily yield hydrogenated films, this preparation technique allowed us to separate the roles of nitrogen and hydrogen in the observed properties. Hydrogen has been introduced in the gas mixture for some samples. The films are a few μm thick and the deposition rate was between 0.6 and 4 μm/h depending on the percentage of Ar in the mixture. The deposits have been made during each run on different substrates such as corning glass and/or quartz for optical transmission measurements, single Si discs for X ray diffractometry, alumina for high temperature annealing ($>1200^\circ$C)and copper grids covered with holey carbon for Transmission Electron Microscopy (TEM). The heat treatments were performed under an Ar flux, at temperatures of 1000,1200,1300, and 1400°C.

3. Measurement of the film compositions

The composition of the films (in particular the C/N ratio) was varied by changing the partial pressure of N_2 in the $Ar + N_2$ total pressure. Since C and N atoms are both light and close elements in the periodic table they are difficult to quantify by Energy Dispersive X ray Spectroscopy (EDXS), in particular with Cameca Electronic Microprobe (EPMA). In order to check the EPMA composition measurements performed on thick samples we have prepared in the same run, very thin films which were simultaneously analysed by Energy Loss Spectroscopy (EELS) and EDXS in a JEOL TEM 2000 FX microscope run at 200 kV. Two SiCN films ($N_2/(N_2 + Ar) = 0.2$ and 0.8) have been analysed in the microscope equipped with Si : Li EDXS Oxford and Gatan PEELS 666 detectors. Si-K, C-K, O-K, N-K characteristic peaks and Si-L, O-K, C-K, N-K absorption edges were chosen for EDXS and EELS respectively. Thin standard specimen have been prepared for elemental quantification to determine the Cliff-Lorimer k factor (EDXS) and the inelastic scattering cross section ratio (EELS). Usual absorption correction (EDXS) and multiple scattering effect (EELS) have been taken into account, depending on the film thickness. In order to compare with the EPMA results, large beam sizes were used (1 μm) in the TEM analyses. The results given by the 3 techniques are gathered in Table I. The comparison between them can be done on the richest N sample number VI. The compositions of the very thin films issued from EDXS and EELS are similar (0.38 and 0.33 for the C/N ratio). This is also the case for the other samples. But the EPMA result on the thick film n°VI exhibits an important deficit in carbon ($C/N = 0.18$). Taking into account the similarity of the EDXS and EELS results in the microscope the significant discrepancy with EPMA can only be explained by an actual difference in composition between thick and very thin samples (very short time of deposition on grids at the beginning of the run). A drastic difference is also concerned with an important oxygen content in the very thin films. This is due to the surface oxidation that dominates the composition, when the surface/volume ratio becomes important. Also shown are the C/N and C/Si ratios. One can see that the N content in the samples increases more rapidly than the percentage of N_2 in the plasma. Another feature of the composition evolution is the C/Si ratio that diminishes drastically with the N content.

4. Techniques of characterisation

4.1. Wide angle X ray diffraction (WAXS)

The spectra have been recorded using a curved detector INEL The sample was placed at the center of the goniometer at a fixed angle with respect to the incident beam. The spectra were recorded by reflection under a low incidence i.e about 5 degree. The range of observation in $Q = 4\Pi\ \sin\vartheta/\Lambda$ was ranging from $Q = 1$ to 7 $Å^{-1}$, using the Co Kα radiation. The whole system was under vacuum, in order to eliminate the diffuse scattering by air. The recording time necessary for an acceptable statistic (1%) was 1000 seconds.

4.2. X ray absorption near edge structure (XANES)

The XANES spectra have been obtained at LURE in Orsay on the SA 32 beam line equipped with a double crystal (InSb (111) monochromator) that allows an energy resolution of 0.7 ev. The super-ACO storage ring was operating at 800 Mev with a typical current of 200 mA. The incident beam was monitored by

TABLE I Composition of the samples. For details see text

SiCN sample numbers	% N_2 in plasma ($N_2 + Ar$) type of target	Techniques A: EPMA B: EDXS C: EELS	Composition					
			Si% (at.% SiCN)	C% (at.% SiCN)	N% (at.% SiCN)	C/N ratio	C/Si ratio	O% (at.% SiCNO)
SiC	0	B	47	53			1.13	
	SiC	C	47	53			1.13	
I	0.5	A	45.52	54.05	0.44	≥100	1.19	≈0
	SiC							
II	1	A	36	30	34	0.88	0.83	≈0
	SiC							
III	5	A	32	21	47	0.45	0.65	≈0
	SiC							
IV	10	A	31	19	50	0.38	0.61	≈0
	SiC							
V	20							
	SiC	B	26	29	45	0.64	1.1	10
		C	21	29	50	0.58	1.43	8
VI	80	A	22	12	66	0.18	0.54	
	SiC	B	24	21	55	0.38	0.87	11
		C	26	18	56	0.33	0.72	20
SiN	10							
	Si	B	39	0	61			
		C	35	0	63			

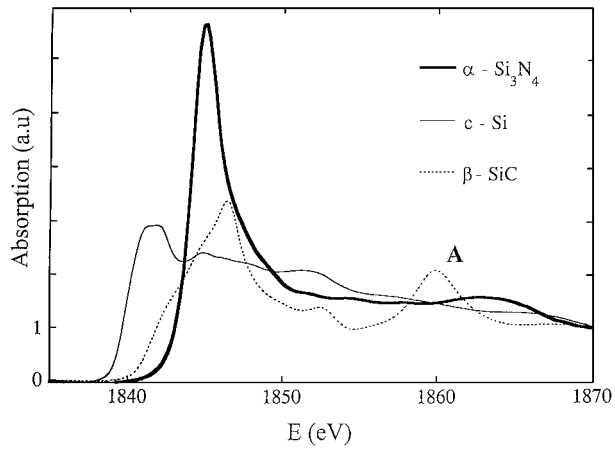

Figure 1 XANES absorption spectra of crystalline Si and Si based compounds. The absorption edges shift towards high energies with the bonding strength. Note the peculiar profile of the c-SiC edge with its shoulder and the strong resonant peak at 1860 ev.

measuring the total electron drain current on a polymeric foil coverd by 2000 Å of Ti located downstream the monochromator. The absorption spectra were recorded in the Total Electron Yield (TEY) mode. The absorption edge energy measured at the inflexion point of the edge is linked to the bonding energy between first neighbours. In Fig. 1, one can see that the edges shift as expected with the bonding strength from Si to SiC, and Si_3N_4. These compounds have been used as references for the SiCN spectra.

4.3. Optical spectroscopy

The transmittance spectra $T(\lambda)$ of the thin films deposited on silica substrates have been recorded by using a Cary spectrophotometer. These spectra allow the determination of the film thickness, refraction index and absorption coefficient as a function of wavelength. In the low absorption range, the existence of interference fringes makes it possible to determine separately the refraction index $n(\lambda)$ and the absorption coefficient $\alpha(\lambda)$ from the transmittance spectrum $T(\lambda)$ only. The vanishing of these interference fringes at higher photon energy due to an increasing absorption coefficient makes it necessary to introduce a second relationship between the two unknown values of $n(\lambda)$ and $\alpha(\lambda)$. This relationship is the Ketteler-Helmholtz relation between the real (n) and imaginary (k) parts of the complex index, developed as a function of $1/\lambda^2$:

$$n^2 - k^2 = A_0 + A_1/\lambda^2 + A_2/\lambda^4 + \cdots$$

$\alpha(\lambda)$ and $k(\lambda)$ are related by

$$\alpha(\lambda) = 4\pi k(\lambda)/\lambda$$

The constants A_i are fitted from the experimental values of n and k in the low absorption range.

While this proved reliable method leads to consistent results for the binary compounds (a-SiC, a-SiN), it yields anomalous results for the ternary compounds (a-SiCN) at thigh photon energy such as a drastic decrease of n with increasing photon energy when constant or increasing values are expected.

In order to check this anomalous behaviour, we have performed ellipsometry measurements. The comparison between the values of n obtained by the two techniques is shown in the insert of Fig. 2, for a film whose Nitrogen atomic content is about 45% (sample III) The discrepancy observed between the n values extrapolated from the transmittance measurements in the low energy range and the ellipsometry data reveals the failure of the transmittance method. Nevertheless, despite the anomalous decrease of n below the values given by ellipsometry it can be seen in Fig. 2 that the values of k obtained to fit the transmittance data (up to the maximum sensitivity of the apparatus) are very close

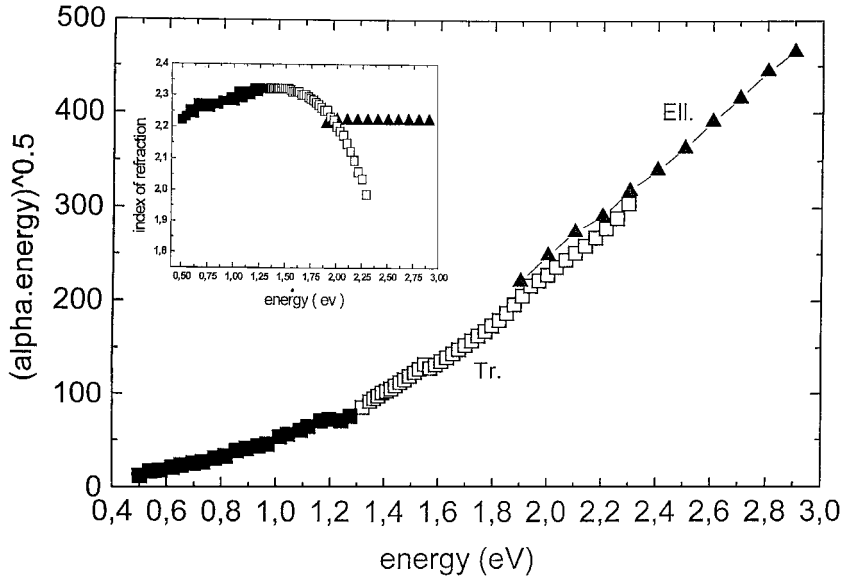

Figure 2 Inset: refraction index of sample III. Open squares: values obtained by extrapolation of n measured in the low energy range (solid squares). Solid triangles: values obtained by ellipsometry. Tauc's plots of the optical absorption versus energy of sample III (47% of nitrogen) obtained by transmittance measurements (Tr.: squares) and Ellipsometry (Ell.: triangles). Open and solid squares correspond to the values of n in the inset.

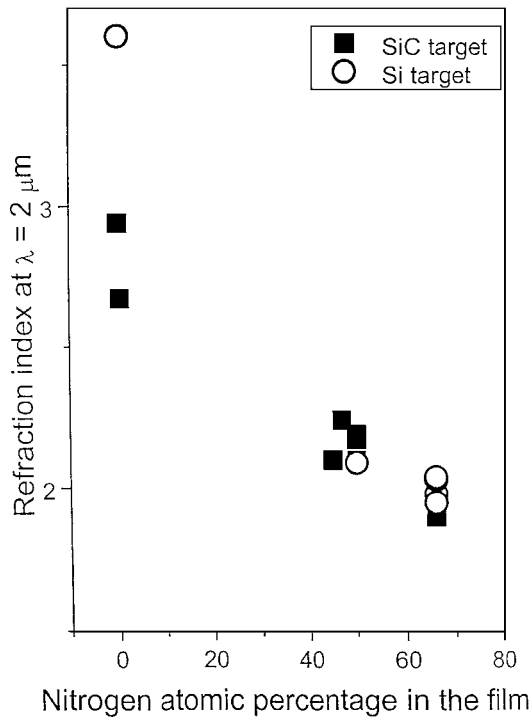

Figure 3 Refraction index of the sputtered a-SiCN films in the low energy range ($\lambda = 2\ \mu$m) as a function of the nitrogen atomic percentage in the film when sputtering either a Si target or a SiC one.

to the ellipsometry ones in the intermediate range from 1.9 to 2.3 ev.

Fig. 3 highlights the cause of the failure. It shows the unambiguous refraction index n value at low photon energy ($\lambda = 2\ \mu$m) as a function of the nitrogen percentage in the sample when using either a SiC or a pure Si target. It can be seen that a low percentage of nitrogen in the sample is sufficient to drastically decrease the refraction index n from its initial value (a-Si or a-SiC) to a value which is independent of the carbon content in the film.

It appears from these results that the refraction index in the high nitrogenated films is controlled by the Si-N bond while the absorption coefficient is controlled by the Si-C bond, leading to an inconsistent application of the Ketteler-Helmholtz relation mentioned above. Beside the failure of the transmittance method for most of the ternary compounds, one will note its success in the case of low nitrogenated films (sample I) as a signature of an homogeneous "solid solution" between the three elements.

5. Results and discussion

5.1. Effect of the introduction of N atoms on the local atomic order of a-SiC

The association of SiC and Si_3N_4 as already mentioned, can be realized either at a macroscopic scale (a composite material) or at the atomic scale (hybridization). Regarding X ray diffraction, the spectrum of a composite material is obviously the sum of the individual spectra of the constituents. But what should be the spectrum of an hybridized SiCN material? We know that the typical diagram of a tetracoordinated compound such as a-SiC is constituted of 2 main haloes up to $Q = 5$ Å^{-1}, followed by others rapidly decreasing in intensity. It has been shown [11], that the second halo near 4.3 Å^{-1} is ruled by the first neighbour interatomic distance, that represents, coupled with the second interatomic distance within one elementary tetrahedron, the Short Range Order (SRO) of the disordered network. The first halo near 2.4 Å^{-1} called in [11] the "prepeak" of the previous one, is concerned with the Medium Range Order (MRO), that is built up by the connectivity of tetrahedra between each others (dihedral angle statistics). In the case of a-Si_3N_4, the mixture of four fold coordination (Si environment) and three fold one (N environment) generates a complex prepeak with 2 components from 1.8 to 3.5 Å^{-1}. We shall focus first on the SRO behavior (2nd halo) with the increase of N content and a further look will be devoted to the MRO through the analysis of the 1.8–3.5 Å^{-1} domain.

5.1.1. Short range order (SRO) in the SiCN films

The 1st neighbour distance associated peak of the Si_3N_4 XRD diagram is at 4.8 $Å^{-1}$ instead of 4.3 for a-SiC, since the Si-N close neighbour distance is shorter (1.74 Å) than the one in a-SiC (1.89 Å). Therefore the sum of the 2 spectra for a composite SiCN material should exhibit 2 second haloes at 4.3 and 4.8 $Å^{-1}$. But since they are very broad, they actually overlap. It results in a vanishing of the 2 components, forming a continuous background that will be the case for annealed samples as seen in Fig. 7. Now let us conjecture that an "alloy" of SiCN composed of mixed tetrahedra should present a clear unique 2nd halo which location in Q will depend on the N content. Indeed the Si-C and Si-N 1st interatomic distances ought to relax when gathered in one tetrahedron. This is favored by the bonding of N atoms that are in substitution sites (for low contents) with a four fold coordination. This is what can be verified in Fig. 4. The positions of the 2nd maxima are marked by arrows and vary with the composition as verified in the inset of the figure. The shift is roughly linear with the N content, up about 50% and decreases slowly afterwards up to the SiN binary compound. This maximum can be explained by the existence of C-N distances smaller than the Si-C and Si-N ones, about 1.5 Å(hence larger Q). Nevertheless the 2nd haloes are less marked in ternary samples than in binary materials (see for example the SiN spectrum). They appear as bumps emerging from a monotonous background; this is particularly visible in the case of sample IV with a very broad maximum divided perhaps in 2 components? We conclude from these observations that the local order is heterogeneous with zones of mixed and demixed tetrahedra.

The XANES results will reinforce this hypothesis. They are gathered in Fig. 5. We have seen that the profile of the absorption edge for pure a-SiC is different

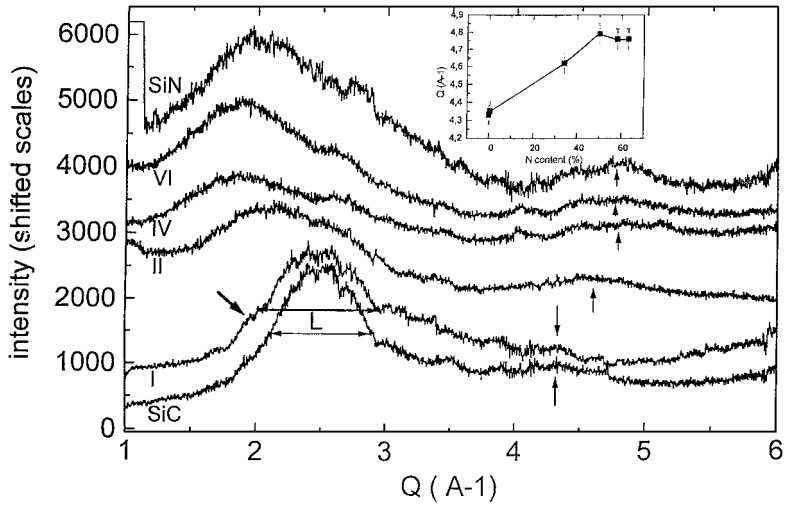

Figure 4 X ray diffraction spectra for increasing N content from bottom to top. The number are those of Table I for SiCN samples. SRO: the arrows mark the maximum of the 2nd peak. It's location in Q versus N content are reported in the inset. MRO: Note the increasing intensity of the typical prepeak of the nitride near 1.8–2 $Å^{-1}$. The thick arrow shows the emergence of this peak in sample I. The disorder induced by N atoms enlarges the FWHM (L) of the 1st peak of SiC (horizontal arrows).

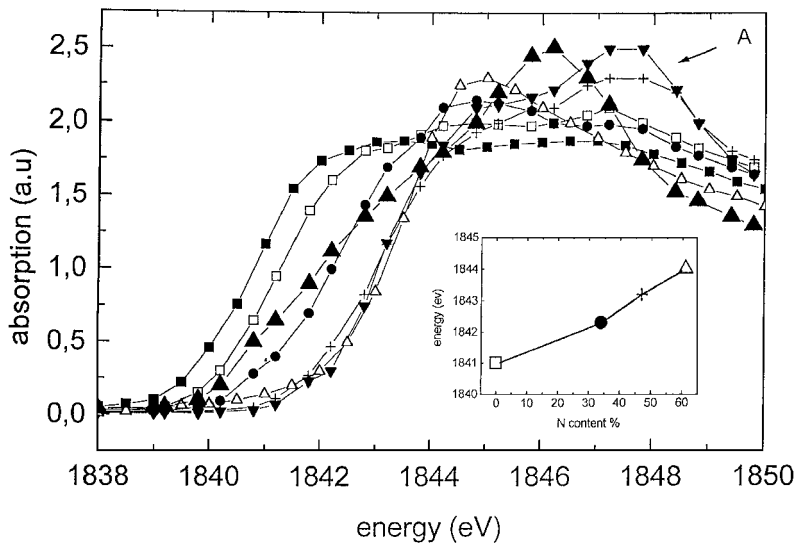

Figure 5 XANES spectra (from left to right): a-SiC (solid squares); a-SiCN I (open squares); c-SiC (solid up triangles); a-SiCN II (solid dots); a-SiCN III (crosses); a-SiCN V (solid down triangles); a-SiN (open up triangles). Inset: Energy values of the absorption edges versus N content. The letter A indicates oxydation peaks.

from its crystallized counterpart also shown in Fig. 5. The position in energy of the 2 edges are the same at 1841 ev but the amorphous curve does not exhibit an inflection above the first edge, like in the crystalline spectrum. Theoretical calculations of the edge profile of c-SiC aggregates [12], involving diffusion paths in spherical clusters, have shown that the particular feature of the edge as well as the resonant A peak in the EXAFS domain (see Fig. 1) appear when a 7th shell of atoms is added to the cluster. Its size is now 1.2 nm and it contains 87 atoms. It is interesting to remark here that the distinction between the amorphous and the crystalline states by XRAD begins also for a crystal size of 1.5 nanometer with a splitting of the 2nd halo into the (220) and (311) lines of the diamond structure.

As far as SRO is concerned, the profile of the XANES absorption edge of a mixture of SiC_4 and SiN_4 tetrahedra is necessarily a compositionally weighted sum of the 2 individual spectra of crystallized SiC and Si_3N_4. This sum will exhibit 2 fixed edge energies whatever compositions provided that their crystal sizes are at least 1.5 nm in diameter. An homogeneous amorphous matrix containing only mixed tetrahedra will have a unique absorption edge which position in energy will shift linearly with composition. Always by comparison with X ray diffractometry this evolution is similar to the shift of the second halo and has the same signification i.e. an apparent averaging of the 1st neighbour distance of Si-C and Si-N when regrouped in the same tetrahedron. One can see in Fig. 5 that the energies of the edges for SiCN samples have a unique value increasing with the N content. In the inset we show this evolution. The variation is almost linear and the deviation from proportionality is a measure of the degree of heterogeneity, i.e a mixture of mixed and demixed tetrahedra zones. The equivalent proof in X ray spectra is represented by the simultaneous presence of the complex first "prepeak" of the nitride connectivity between 1.8 and 2.5 $Å^{-1}$ (3 fold coordination for N) and the 2nd halo emerging from the background (4 fold coordination).

5.1.2. Medium range order (MRO) in the SiCN films

The first halo of the a-SiC diagram lies at 2.45 $Å^{-1}$. It corresponds to a "prepeak" of the peak ruled by the 1st neighbour interatomic distance in tetracoordinated material (SiC_4) The equivalent prepeak for the nitride (SiN_4) lies at 2.6 $Å^{-1}$ (since Si-N is shorter than Si-C). This is the 2nd component of the complex prepeak of the a-Si_3N_4 spectrum. The first component lies at 1.8 $Å^{-1}$ and is generated by the 3 fold coordination of N (NSi_3) (called "prepeak bis" in [11]). It characterizes the local nitride topology. It follows that if N atoms occupy substitution sites in the network of a-SiC with a coordination 4 no peak should be expected near 1.8 $Å^{-1}$. The progressive nitridation is revealed by the increase of the intensity of the halo near 1.8 $Å^{-1}$, going in Fig. 4 from bottom to the top. The local heterogeneity is already visible in the spectrum of sample I (about 0.5% of N) with a slight shoulder near 2 $Å^{-1}$. The Ful Width at Half Maximum (FWHM) of the halo of sample I is significantly larger than the one for a-SiC. It is a mark of greater local disorder. Recalling what has been developed in the SRO paragraph one can infer that while the presence of one and only one second halo in the SiCN system reveals an homogeneous phase with mixed tetrahedra with a 4 fold topology for N environment, the existence of a peak near 1.8–2 $Å^{-1}$ reveals conversely a nitride like phase with demixed tetrahedra and a coordinence 3 for N. The simultaneous presence of both peaks is the signature of a locally heterogeneous local order.

5.2. The relationship between optical properties and local atomic order in the amorphous films

Alike in the a-Si case, non hydrogenated a-SiCN materials contain many dangling bonds and other optically active defects that generate band tails responsible for optical transitions below the absorption edge. Consequently the slopes of their absorption edge are not so steep as those of hydrogenated materials. The Tauc's plots $(\alpha h\nu)\hat{}0.5$ are gathered in Fig. 6. We have not reported the results for all compositions for the sake of clarity because up to sample V composition, the absorption edges are almost superposable. They remain close to that of pure SiC meaning that the SiC bonds dominate α. Unhydrogenated samples, as expected, exhibit a relative important absorption below the gap which cannot be precisely determined by extrapolation down to the energy axis. However the SiN gap is easy to determine (4.3 ev), lower than the Si_3N_4 one (about 5 ev).

The subgap absorption is due to band tails generated by disorder. The amorphicity is by itself a source of disorder through bond angle and bond length fluctuations, but also there is a chemical disorder issued from compositional inhomogeneties such as mixed and demixed tetrahedra zones, already invoked to explain the X ray spectra. Nevertheless, sample III, the spectrum of which is treated in Fig. 2 is likely very heterogeneous since the transmittance method fails to give plausible values for the index of refraction in the high absorption range.

The X ray analysis has shown that the Si-C and Si-N interatomic distances are modified in mixed tetrahedra. Since the gap value is at least qualitatively a function of the interatomic distance we had conjectured that an homogeneous material containing only mixed tetrahedra should have its specific dielectric function and absorption edge associated with a gap linearly dependant with N content. The fact that up to 50% of N, the edge is almost pinned in the same region not far from the SiC one, indicates that the material is heterogeneous with large demixed tetrahedra zones. This hypothesis will be reinforced by the annealing effect on sample I [10, 11].

5.3. Variation of the local order and optical properties with annealing

One major goal of the search of new ceramics has been the increase of the crystallization temperature of a-SiC in order to keep the good mechanical properties of the amorphous state at temperatures approaching 1500°C. Recently many attemps have been done towards this

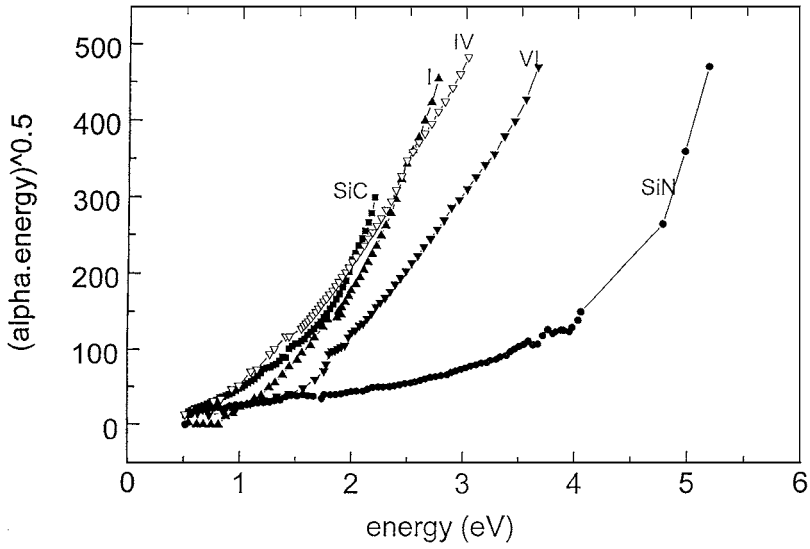

Figure 6 Optical absorption spectra for increasing N content. The absorption edges of SiCN samples are close to the a-SiC edge up to 50% of N in sample IV. A significative shift is obtained for 66% in sample VI. The slope of the edges are not steep due to large band tails. The gap of the SiN film is about 4.3 ev narrower than the gap of the Si_3N_4 one.

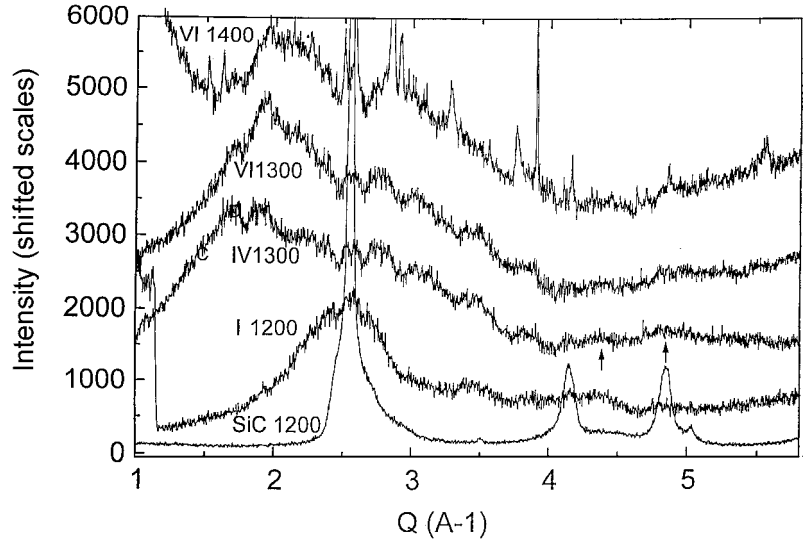

Figure 7 X Ray Diffraction spectra of annealed samples. Pure SiC is fully crystallized (α and β phases) at 1200°C while sample I is still amorphous. SRO: The unique 2nd peak of the spectra of Fig. 4 have disappeared except for sample I. Even, the arrows mark the emergence of the haloes of a-SiC and a-Si_3N_4. MRO: At 1300°C samples IV and VI are still amorphous but large ripples appear, revealing the nucleation of the equilibrium phases SiC and Si_3N_4 that appear at 1400°C (narrow diffraction lines).

objective [13, 14]. The materials are issued from the decomposition of organo-silicon precursors. The T_c of hybridized SiCN "alloys" has been maximized up to 1500°C for a composition close to $Si_6C_3N_4$ i.e. for an average number of first neighbors for Si equal to 2 C and 2 N atoms [15, 16]. In the following we intend to investigate the effect of the demixion under annealing on the local order and optical properties.

5.3.1. X ray spectra

The spectra of the annealed samples are shown in Fig. 7. Amorphous pure SiC begins to crystallize already at 1000–1100°C. At 1200°C the result is a mixture of the cubic β phase and the hexagonal α phase. The crystallization temperature of a-SiC is significantly increased by a very small amount of nitrogen. This is what occurs for sample I containing about 0.5% of N that does not crystallize at 1200°C. The comparison with the as deposited spectrum in Fig. 4 shows that the shoulder on the left side of the first halo has disappeared, meaning that the nitride like zone have transformed into a carbide like connectivity. Accordingly, there is a change of the coordination from 3 fold to 4 fold topology. Simultaneously the FWHM diminishes revealing a relaxation of the MRO.

The second halo is still present and even reinforced. Conversely the second peak of the SiCN IV spectrum is after annealing at 1300°C, clearly divided into 2 subpeaks maxima at 4.3 and 4.8 $Å^{-1}$ instead of a very broad unique maximum for the as deposited sample. The demixion is achieved. Along the MRO domain the spectrum exhibits a series of ripples which can be interpreted as enlarged diffraction lines of the α Si_3N_4 phase that will appear at 1400°C. At 1300°C the spectrum of

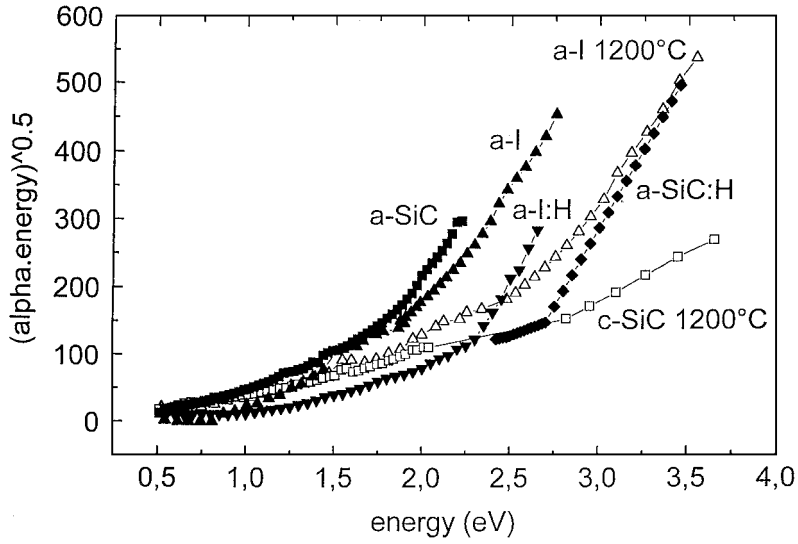

Figure 8 Optical absorption spectra of annealed samples. The SiC spectrum after annealing at 1200°C reveals its crystallization while the Sample I (0.44% of N) is still amorphous. The effect of relaxation shifts drastically the edge towards higher energy and reduces the sub gap absorption. For comparison the effect of about 10% of hydrogen is shown in I (H), our sample and in a-$Si_{55}C_{45}$: H after Stuzmann *et al.* [7].

the sample VI presents the same ripples as those of sample IV, indicating that they are not produced by a noisy background but rather by the lines of a nanometric crystalline phase. Indeed the width of the lines must be sufficiently large to overlap.

Such enlargement is estimated to correspond to a grain size of about 3–5 nanometers. The nucleation of nitride germs requires a diffusion process of atoms, to destory the mixed tetrahedra and change the N sites from 4 fold to 3 fold connectivity. It is the inverse evolution of the one occuring in the sample I at 1200°C. This apparent contradiction can be explained by the very low N content in sample I. The distance between 2 N atoms is large enough to exclude the formation of the nitride topology. Their rearrangements in sample I favors the relaxation of the disordered network of a-SiC.

5.3.2. Optical characteristics

The optical spectra of the annealed films shown in Fig. 8 reflect the evolution already detected by XRAD. The drastic change of the spectrum of a-SiC after its crystallization at 1200°C recall the well known transition from the amorphous to the crystalline state of Si that has been the object of a considerable amount of works. Mainly the very important decrease of the slope of the absorption edge that reduces drastically the sub-gap absorption near 2 ev. In contrast the slope of the absorption edge of sample I does not change after annealing confirming that it is still amorphous. Surprisingly there is an important shift of the edge parallelly to itself. Meanwhile the optical gap increases from about 1.6 ev to 2.4 ev. It is worth saying that the transmittance method is here applicable up to 3.5 ev demonstrating that the heating at 1200°C does not provoke the formation of a biphased material. The amount of nitrogen about 0.5% cannot explain by itself such important widening of the gap. It is clearly the indirect effect of the network relaxation already detected by XRD. Hence the important comparison to be done is with the effect of hydrogen. We have prepared an hydrogenated counterpart of sample I by introducing 10% of H_2 in the plasma gaz mixture. The resulting spectrum is shown in the figure together with a a-$Si_{55}C_{45}$: H one after Sussman *et al.* [17]. Besides the shift of the edges hydrogen reduces more efficiently the subgap absorption than the N atoms do between 1 to 2.5 ev. This is explained by the neutralization of the dangling bonds by hydrogen with its higher concentration (10%) than N (0.5%). The value of the gap about 2.1 ev is common to the hydrogenated and nitrided sample The difference in the gap width of a-SiCN : H is likely due to a different C/Si ratio.

The interest of the nitridation is 2 fold. Firstly a very small content of N atoms (less than 1%) gives almost the same effect than about 10% of hydrogen. Secondly the amorphous state is stabilized at 1200°C a temperature that should provoke the complete effusion of hydrogen and the crystallization of a-SiC.

The optical spectra of N rich samples could not be measured by transmission. The annealing at 1200°C prior to crystallization increases the heterogeneity of the local order and the transmittance method fails completely above 1.5 ev. There is no possible solution for the n, k determination from the extrapolation method in order to fit the experimental transmission data, even with an anomalous drastic decrease of n like in the as prepared samples. We emphasize here the parallelism between the effect of the destruction of the hybrid SiCN phase on the atomic MRO and the definitive failure of the refraction index determination by the transmittance method. The change of MRO is associated with the change of coordination for N atoms from 4 to 3 inducing a local decrease of the density (8 membered rings in Si_3N_4 instead of 6 in SiC) and hence a decrease of the index of refraction. XANES results for annealed films are severly perturbated by oxydation since this method explores mainly the surface of the sample. Unfortunately the measurements by ellipsometry were not also possible due to an excessive roughness of the sample surface after heating.

6. Conclusion

We have shown in this study that the RF cathodic reactive sputtering enables us to prepare amorphous, unhydrogenated a-$Si_xC_yN_z$ films, hybridized at the nanometric scale. However there is still 2 possible manners of chemically assembling the 3 atoms inside a volume of 1.5 nm in diameter containing about 80 atoms. Our goal has been to describe the micro structure inside this volume and follow its modification under heating. The important result is that the as prepared films are structurally and chemically heterogeneous. The 2 techniques of characterization, WAXS and XANES have brought about coherent results in that direction at least at a qualitative level: an heterogeneous disordered matrix containing zones of a-Si-C-N solid solution and zones were demixed tetrahedra form already a composite material. Note that for the sake of simplification we have deliberately omitted other types of bonding such as Si-Si or C-C bonds that are likely present in the material.

On the XRD side the Fourier transform of the experimental interference function leading to the Radial Distribution Function (RDF), should have given quantitative values on the mean interatomic distances values and the coordination numbers, but in the mean time the RDF being a pair function cannot tell us how the Si-C and Si-N pairs are locally assembled in mixed or demixed tetrahedra. We have seen that the unique 2nd peak of the XRD spectrum reveals effectively the 2 kinds of assemblage of mixed tetrahedra. In that aspect the reciprocal space informations are competitive with the XANES results. The averaging of the distances within one mixed tetrahedron (unique 2nd peak of XRD) modifies also the charge transfer between first neighbours revealed by the shift in energy of the Si 1s level absorption edge (XANES). The same parallel can be made between the capacity of the 2 techniques to detect the formation of crystallized nuclei. The critical size of 1.5–2 nm is the same for the split of the 2nd halo of the X ray spectrum into the 220 and 311 lines and the modification of the profile of the XANES edge as well as the resonant peaks in the EXAFS domain.

The optical absorption is also sensitive to the change of local chemical homogeneity. The complex dielectric function is linked to the bonding strength (SRO), and the local density (MRO) that are different in mixed or demixed tetrahedra zones. The imaginary part of the dielectric function should only be determined, in this last case, by the effective medium modelization.

The lowering of entropy due to relaxation increases significantly the crystallization temperature of a-SiC even with less than 1% of N content. The absence of hydrogen in our samples allowed to point out the relaxation role of nitrogen during the annealing stage at 1200°C. The resulting important shift of the optical absorption edge from 1.6 to 2.4 ev that have been clearly attributed to the network relaxation is perhaps the most interesting result of this study.

References

1. G. SASAKI, H. N. NAKASE, K. SUGANUMA and T. NIIHARA, *J. Ceram Soc. Jpn.* **100**(4) (1992) 536.
2. F. ROSSIGNOL, P. GOURSAT, J. L. BESSON and P. LESPADE, *J. Eur. Ceram. Soc.* **13** (1994) 299.
3. K. NIIHARA, T. HIRANO and K. IZAKI, *Ceramic Transactions, Am. Ceram. Soc. Inc.* **42** (1994) 207.
4. J. L. BESSON, M. MAYNE, D. BAHLOUL-HOURLIER and P. GOURSAT, *J. Eur. Ceram. Soc.* **18** (1998) 1893.
5. F. WAKAI, Y. KODAMA, S. SAKAGUCHI, N. MURAYAMA, K. IZAKI and K. NIIHARA, *Nature* **344** (1990) 421.
6. T. ROUXEL, F. WAKAI and K. IZAKI, *J. Amer. Ceram. Soc.* **75**(9) (1992) 2363.
7. M. DUCARROIR, W. ZHANG and R. BERJOAN, *J. de Phys. IV, Coll. C3, J. Phys. II* **3** (suppl.) (1993) 247.
8. K. KAMATA, Y. MAEDA and M. MORIYAMA, *J. Mater. Sci. Lett.* **5** (1986) 1051.
9. I. NAKAAKI, N. SAITO, Y. INUI, S YOSHIOKA and S. NAKAMURA, *Phil. Mag.* B **68**(1) (1993) 55.
10. N. SAITO, T. GOTO, Y. TOMIOKA, T. YAMAGUCHI and M. SHIBAYAMA, *J. Appl. Phys.* **69**(3) (1991) 1518.
11. J. DIXMIER, *J. Phys. I, France* **2** (1992) 1011.
12. P. SAINCTAVIT, J. PETIAU, C. LAFFON, A. M. FLANK and P. LAGARDE, in "X ray Absorption Fine Structure" edited by S. Shasnain (E. Horwood, New York, 1991).
13. M. CAUCHETIER, O. CROIX, N. HERLIN and M. LUCE, *J. Amer. Ceram. Soc.* **74** (1994) 1142.
14. D. MOCAER, R. PAILLER, R. NASLIN, C. RICHARD, J. P. PILLOT, J. DUNOGUES, C. GERARDIN and F. TAULELLE, *J. Mater. Sci.* **28** (1993) 2615.
15. J. DIXMIER, R. BELLISSENT, D. BAHLOUL and P. GOURSAT, *J. Eur. Ceram. Soc.* **13** (1994) 293.
16. F. TENEGAL, B. BOUCHET, R. BELLISSENT, N. HERLIN, M. CAUCHETIER and J. DIXMIER, *Phil. Mag.* A **78**(4) (1998) 803.
17. R. S. SUSSMANN and R. OGDEN, *Phil. Mag.* **44** (1981)(1) 137.

Received 24 May 2001
and accepted 25 February 2002